Desalination and Water Treatment
www.deswater.com
doi: 10.5004/dwt.2022.28818

272 (2022) 167–182
October

Adsorption of humic acid onto chitosan polyvinyl alcohol blend membrane from solution and second adsorption toward copper ions

Yuting Ma, Rong Wang*, Chenghui Ma, Runping Han*

College of Chemistry, Zhengzhou University, Kexue Dadao #100, Zhengzhou, China 450001, emails: wangjoya@zzu.edu.cn (R. Wang), rphan67@zzu.edu.cn (R. Han), 202012152012632@gs.zzu.edu.cn (Y. Ma), 1427519817@qq.com (C. Ma)

Received 27 April 2022; Accepted 11 August 2022

ABSTRACT

Chitosan (CS) and polyvinyl alcohol (PVA) have been widely used due to their unique structures. In this study, chitosan (CS) and polyvinyl alcohol (PVA) were blended to prepare CS-PVA membrane, which was used to study the adsorption performance of humic acid (HA). Then, CS-PVA-HA membrane was obtained to study the adsorption performance of copper ions. The two membranes were characterized by isoelectric point (pH_{pzc}), Fourier-transform infrared spectroscopy, scanning electron microscopy and X-ray photoelectron spectroscopy, and the adsorption mechanism was investigated respectively. The adsorption results showed that the adsorption capacity of HA by CS-PVA could reach 111 $mg \cdot g^{-1}$ at the optimal pH value of 6. Langmuir model was suitable to describe the equilibrium adsorption process, and pseudo-second-order kinetic model was used to predict the kinetic adsorption behavior of CS-PVA toward HA. The data adsorption of HA on CS-PVA membrane was a spontaneous exothermic adsorption process. When the optimal pH value was 5.5, the adsorption capacity of Cu^{2+} on CS-PVA-HA membrane was 85.0 $mg \cdot g^{-1}$. Freundlich model was suitable to describe the adsorption process, and Elovich equation could better describe the kinetic adsorption behavior of Cu^{2+}. The adsorption was a spontaneous endothermic process. The prepared composite material had good adsorption performance and could be used to remove the corresponding pollutants in water.

Keywords: Chitosan polyvinyl alcohol blend membrane; Adsorption; Humic acid; Copper ion

1. Introduction

Humic acids are complexes of large molecules, mainly carbon, oxygen, and hydrogen, with small amounts of nitrogen, and occasionally phosphorus and sulfur. Humic acids contain carboxyl, phenolic, carbonyl and hydroxyl groups linked to aliphatic or aromatic carbons. It reacts with chlorine during water treatment to produce the toxic trihalomethane. To reduce the presence of trihalomethane, as much humus as possible must be removed prior to chlorination [1,2]. Yang et al. [3] has studied the effect of humic acid (HA) on the adsorption of copper ion on multilayer reduced graphene oxide (FGO) using batch equilibrium method, Fourier-transform infrared spectroscopy (FTIR) and EXAFS. Research results show that oxygen-containing functional groups and negative charges can be introduced into the surface of FRGO through adsorbed HA, and then chemical complexation and electrostatic attraction can increase the adsorption of Cu^{2+}. Humic acid is one of the main problems affecting water supply in the utilization of water resources, and it is of great practical significance to minimize its presence in drinking water [4]. Adsorption is a promising method to remove humic acid from water [5].

Heavy metal pollution is one of the important problems related to life. Due to the characteristics of long-term

* Corresponding authors.

persistence, bio-enhancement and non-degradation of heavy metal ions in the food chain, they will continue to bioaccumulate along the food chain, and eventually will be enriched in a large number of animals or human bodies, and their content in water resources also gradually increases. When heavy metal ions are transformed from stable components into bioavailable forms, exceeding a certain amount will pose a serious threat to the health of organisms [6]. In short, if excessive metal poisoning occurs in the body, it is difficult to cure. As the primary pollutant, heavy metals have the characteristics of toxicity, persistence and non-degradation, which have aroused people's attention. Although copper is one of the essential elements in the human body, its widespread use can lead to the release of more copper ions into the environment and further into living organisms through various pathways. Copper can not only induce depression, it can also accumulate in the liver, brain and pancreas, causing vomiting, convulsions and even death. Adsorption method has been widely used because of its high efficiency, easy operation and regenerative ability [7,8]. In recent years, many new modified adsorbents, composite adsorbents and multifunctional materials have been prepared and applied to remove metal ions [5,9]. Chitosan is made from industrial waste and is cheap. Due to the existence of functional groups (amino and hydroxyl) in its structure, various types of forces or bonds can be generated, such as van der Waals force, hydrogen bond and ionic force, so as to realize the adsorption process [10,11]. However, chitosan also has low pH sensitivity, poor swelling and small surface area. Wu et al. studied selective adsorption of Cu(II), Pb(II) and Ni(II) metal ions by chitosan/poly(N-isopropylacrylamide) composite hydrogel [12]. The equilibrium adsorption data are in good agreement with the Langmuir model, and the adsorption kinetics data are also in agreement with the quasi-second-order model. Using methyl methacrylate (M-CTS) as adsorbent, Sutirman et al. [13] synthesized a novel crosslinked chitosan that can effectively remove Cu ions from water. Chitosan can improve its mechanical properties by crosslinking. Crosslinking not only improves mechanical properties but also reduces the density of active sites, thus weakening the ability of chitosan to purify water. Therefore, it is very important to find a kind of energy saving and environmental protection material as the support material of chitosan. Simsek et al. [14] made composite films of microporous carbon fibers encapsulated in chitosan-polyvinyl alcohol polymer for the adsorption of BPA from wastewater. Rodrigues et al. [15] used vanadium ions to modify chitosan membranes to improve the adsorption regeneration capacity of chitosan membranes for the removal of reactive black 5 dye from aqueous solutions. The adsorbent composite membrane has a certain regenerative capacity. According to the literature, chitosan can be functionalized by many reagents, including polyvinyl alcohol, alumina, cellulose, cyclodextrin, etc. [16].

In this study, chitosan (CS) and polyvinyl alcohol were co-mixed into CS-PVA and CS-PVA-HA films with high adsorption capacity, which can effectively remove humic acid and Cu^{2+} from solution. Based on the isoelectric point, infrared spectrum, scanning electron microscopy characterization, the adsorption property of membranes toward humic acid and copper was performed and adsorption mechanism was discussed. This experiment is somewhat novel. First of all, the material is simple and easy to obtain, chitosan is produced by the deacetylation reaction of crustaceans or microorganisms, and shrimp and crab shells are the most produced food industry waste in the world. Moreover, the prepared membrane materials are easy to separate and have good adsorption results toward HA and Cu^{2+}. The second adsorption of HA-loaded membrane is some novel for binding copper ions. The final preparation process is relatively simple and does not need to go through cross-linking. Therefore the study has some significance.

2. Materials and methods

2.1. Material

Chitosan (CS), polyvinyl alcohol (PVA), acetic acid, humic acid (HA), copper sulfate, sodium hydroxide, all chemical reagents were analytically pure, and the laboratory water was deionized water.

2.1.1. Preparation of CS-PVA membrane

The adsorbent CS-PVA film was prepared by simple blending method. Fig. 1 illustrates the synthesis steps. Firstly, chitosan was dissolved in 2% acetic acid solution, and ultrasound was performed for 2 h. Then PVA was dissolved in a 95°C water bath to obtain a 5% polyvinyl alcohol solution. The two solutions were then mixed in a 2:1 mass ratio. After the bubbles were eliminated with an ultrasonic instrument, a quantitative volume of mixed solution was added to the petri dish with a fixed surface area, which was tiled and placed on a horizontal platform for air drying. Then, the prepared film was soaked with 2% NaOH solution to make it fall off naturally. The CS-PVA membrane was prepared by washing it with distilled water and then soaking it until the pH value of the solution was neutral.

2.1.2. Preparation of CS-PVA-HA membrane

The CS-PVA membrane prepared in the above process was soaked in humic acid solution with a concentration of 500 $mg \cdot L^{-1}$, placed in a 303 K oscillation box at a constant temperature for 12 h, then removed, washed and soaked with distilled water until the pH value of the solution was neutral, and then dried on a glass platform to prepare CS-PVA-HA membrane.

2.2. Material characterization

Scanning electron microscopy (SEM) (Su8020, Tianmei Scientific Instrument, China) was used to analyze the surface morphology of the two films. X-ray photoelectron spectroscopy (XPS) (Escalab 250Xi, Thermo Fisher, UK) was used to determine the chemical composition of CS-PVA membrane before and after adsorption of HA and Cu^{2+} by CS-PVA-HA membrane. By detecting the pH difference before and after the two membranes, they were plotted with pH_0 respectively, and the isoelectric point was measured. The chemical groups of the two membrane materials were analyzed by Fourier Transform infrared spectrometer (FTIR, Nicolet iS50, USA).

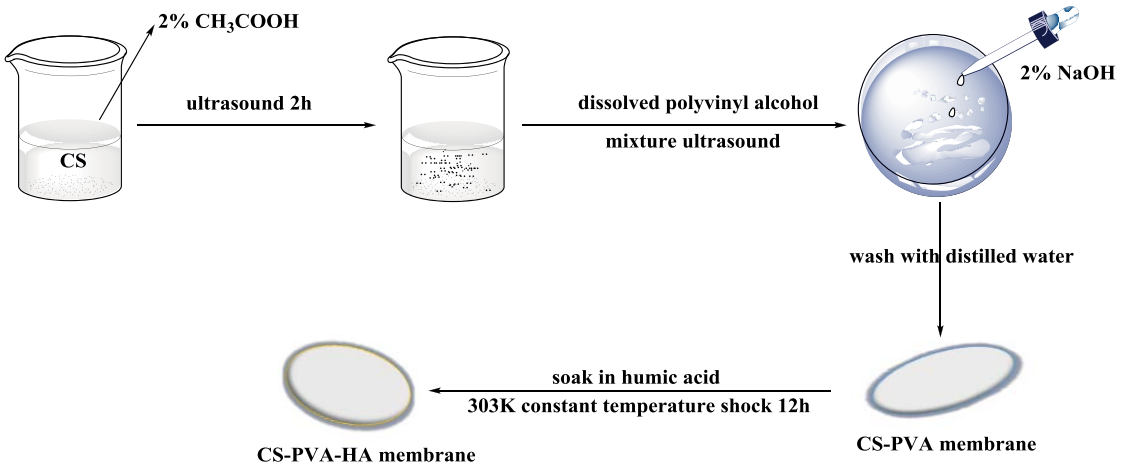

Fig. 1. Preparation process of CS-PVA and CS-PVA-HA.

2.3. Adsorption experiments

The adsorption experiment of HA by CS-PVA membrane was carried out with 50 mL glass sample bottle. Generally, weigh 10 mg CS-PVA and add it to 10 mL HA solution with different concentrations, put it into a constant temperature oscillation box at 300 K. It was taken out after a period of time, and filter to obtain the supernatant. The effects of HA concentration, pH 2–12, temperature 290, 300, 310 K and co-existing ions (0~0.2 mol·L^{-1} NaCl and Na_2SO_4) on the adsorption process were determined. CS-PVA-HA film (8 mg) were respectively weighed into a 50 mL conical flask, and 10 mL Cu^{2+} solution of different concentrations was added, and the adsorption experiment was carried out in accordance with the above method. The adsorption of HA and Cu^{2+} by CS-PVA and CS-PVA-HA was determined by UV-Vis spectrophotometry at 275 nm and 324.7 nm, respectively. Then, the unit adsorption capacity is calculated using Eq. (1).

$$q = \frac{V\left(C_0 - C\right)}{m} \tag{1}$$

where C_0 and C are HA (or Cu^{2+}) concentrations (mg·L^{-1}) in the solution before and after adsorption, respectively. q is the unit adsorption capacity at equilibrium or time t (mg·g^{-1}), p is the removal efficiency (%) of HA (or Cu^{2+}), m is the mass of the prepared film (g), V is the volume of HA (or Cu^{2+}) solution (L). All experiments were repeated two times and average values were recorded.

3. Results and discussion

3.1. Characterization of the prepared materials

3.1.1. Isoelectric point analysis of prepared membrane materials

The pH value of the two prepared films with no charge or zero charge is called isoelectric point. It can be seen from Fig. 2 that not only pH_{pzc} of CS-PVA film and CS-PVA-HA film, but also ΔpH of the two films showed a similar change trend. As pH increases, ΔpH first increases

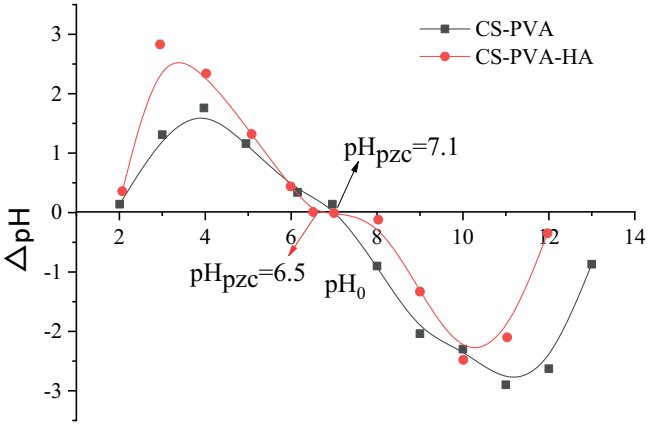

Fig. 2. Changes in the isoelectric point of the material before and after the modification.

and then decreased. When the charge was zero, the isoelectric point of CS-PVA film was 7.1, which may be caused by the dissociation of the basic functional group (amino group) on the surface of chitosan. The isoelectric point of CS-PVA-HA film is 6.5, which may be due to the dissociation of hydroxyl groups on the surface of humic acid, so that the isoelectric point moved to the acidic direction.

3.1.2. FTIR analysis

In order to analyze the functional groups on the surface of two kinds of films, FTIR spectroscopy was usually used to characterize them. Fig. 3 shows FTIR of CS-PVA film and CS-PVA-HA film. There were wide and strong peaks at 3,200~3,600 cm^{-1}, indicating the presence of –OH and –NH_2 groups on the surface of the film [3,17]. This was consistent with peak values at 1,073 and 1,150 cm^{-1}, and belonged to C–O and C–N stretching vibration [18]. The peak located at 1,641 cm^{-1} was characteristic of amine deformation [19]. The peak at 1,380 cm^{-1} corresponded to C–N stretching [20]. There was no change in the wavenumber

of the infrared spectrum loaded by HA to CS-PVA, and no new peak appeared, indicating that there was no significant chemical reaction between the adsorbent and humic acid. Therefore, the adsorption of HA by CS-PVA may contain physical processes. The change in enthalpy during physical adsorption was too small to be sufficient for bond breaking. Therefore, the chemical structure did not change before and after HA adsorption.

3.1.3. SEM analysis of materials

The surface morphologies of CS-PVA and CS-PVA-HA films were investigated by scanning electron microscopy (SEM) at 10000 magnifications. The results are shown in Fig. 4. It can be seen from Fig. 4a and b that the surface of CS-PVA is a smooth and flat film, while the surface of CS-PVA-HA becomes rough. This also increased the contact area of the active site to a certain extent, thus increasing the adsorption effect of Cu^{2+}.

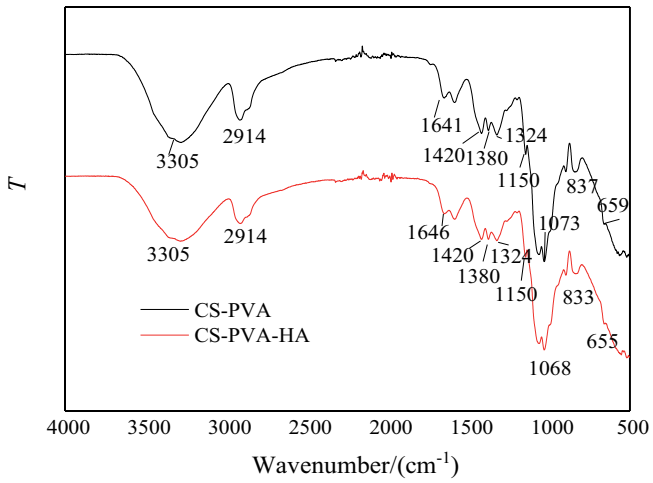

Fig. 3. Infrared spectra of CS-PVA and CS-PVA-HA.

3.1.4. XPS analysis

The mechanism of adsorption of HA by CS-PVA membrane was studied by analyzing XPS diagram (Fig. 5) before and after adsorption of HA by CS-PVA membrane. Since chitosan and humic acid contained the same elements, we further analyzed the peak diagram of XPS. It can be seen from Fig. 6a and b that CS-PVA membrane C 1s can be divided into three peaks: 284.8 eV was C–C, 286.3 eV was C–N (or C–O or C–O–C), 288.1 eV was C=O (or O–C–O), with peak areas of 70.7%, 24.2% and 5.04%, respectively. After adsorption, C 1s also had three peaks, but the peak area ratio was 91.4%, 6.44% and 2.32%. Because C–C adsorbed with humic acid became the main carbon component [21], it indicated that humic acid was adsorbed on CS-PVA film [22,23].

It can be seen from Fig. 6c and d that the CS-PVA film N 1s has only one peak located at 399.4 eV for neutral amino

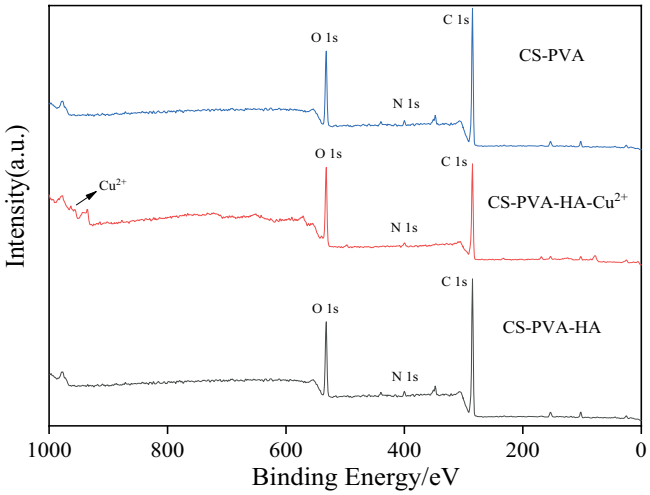

Fig. 5. XPS spectra of CS-PVA (CS-PVA-HA) before and after adsorption of HA (Cu^{2+}).

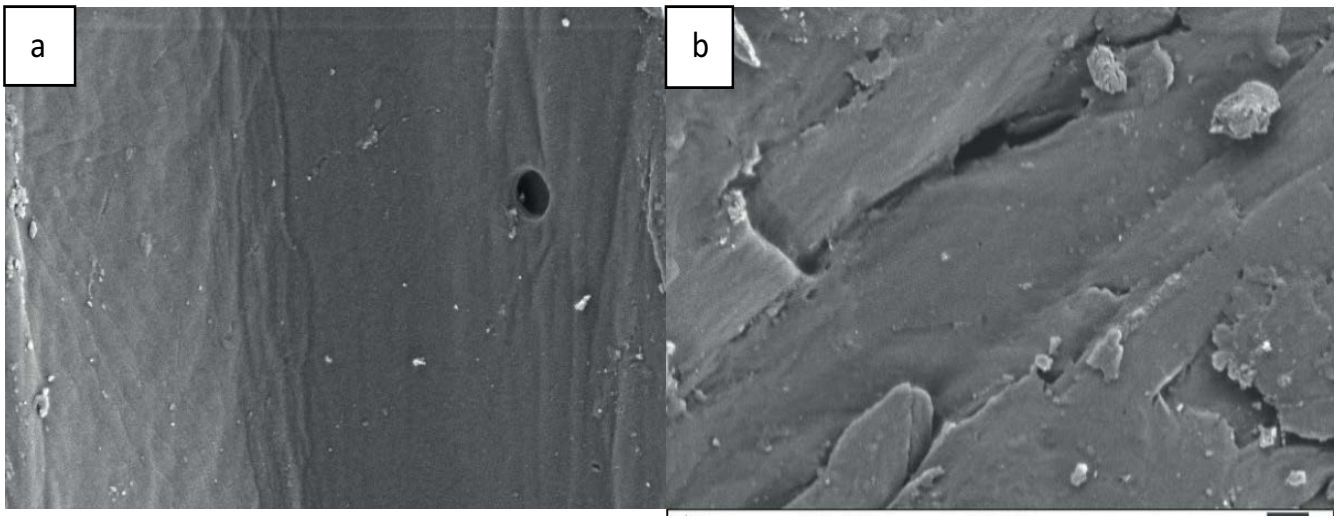

Fig. 4. SEM of both CS-PVA (a) and CS-PVA-HA (b) membranes.

nitrogen (–NH_2) in chitosan. After adsorption of humic acid, a new peak NH_3^+ can be seen in the N 1s spectrum at 403.1 eV, which is caused by the electrostatic gravitational interaction of the amino group in chitosan being protonated with the carboxyl or phenolic group in humic acid [24,25]. Protonation of the amino leaded to a decrease in the relative electron density on the nitrogen atom, thus increasing the binding energy of N 1s [26]. The area of –NH_3^+ peak accounted for 13.5% of the total area, indicating that at least 13.5% amino group forms complexed with humic acid [23]. Another part of NH_3^+ was involved in the adsorption and water formation of NH_3^+–OH, and then becomed –NH_2 again after drying, so the NH_3^+ involved in adsorption should be greater than 13.5%.

The XPS diagram (Fig. 5) of CS-PVA-HA membrane before and after Cu^{2+} adsorption was analyzed to study the mechanism of CS-PVA-HA membrane for adsorption Of Cu^{2+}. It could be seen from Fig. 5 that there was an obvious peak from 925 to 970 eV, indicating that Cu^{2+} had been successfully adsorbed onto the CS-PVA-HA film [27]. In order to study the adsorption mechanism, the XPS peak diagram was further analyzed (Fig. 6). It can be seen from Fig. 6e that Cu 2p of CS-PVA-HA film could be divided into four peaks, three peaks located at 934.9, 938.8 and 934.2 eV correspond to Cu 2p1/2 peak while one peak at 955.2 eV corresponds to Cu 2p1/2 peak. Peaks at 934.9 and 938.8 eV is from COO–Cu^{2+} and Cu^{2+}, respectively, while peaks at 943.2 and 955.2 eV were from CuO [28]. Therefore, it could be inferred that the main adsorption of Cu^{2+} on CS-PVA-HA film was COO^- complexation with HA.

3.2. Adsorption study

3.2.1. Effect of time on adsorption and comparison of CS-PVA and CS-PVA-HA toward Cu^{2+}

The effect of time and dosage on adsorption of HA solution was studied by using CS-PVA membrane as adsorbent. It can be seen from Fig. 7a that CS-PVA film rapidly adsorbed HA in the first 200 min, and then the adsorption rate gradually decreased. This may be because there are a large number of available adsorption sites in the first 200 min. With the progress of the adsorption process, the adsorption sites were gradually occupied, the removal rate increased slowly, and the adsorption reached equilibrium within 360 min (the optimal contact time) [29,30].

The adsorption of Cu^{2+} by time and CS-PVA-HA membrane dosage was studied. The results are shown in Fig. 7b. It could be seen that the adsorption of Cu^{2+} on CS-PVA membrane was significantly lower than that on CS-PVA-HA membrane. The adsorption capacity of CS-PVA-HA membrane was 65.0 $mg \cdot g^{-1}$ and the adsorption capacity of CS-PVA membrane was 3 h. The main reason may be that the addition of humic acid increased the adsorption sites. Because of the complex structure of humic acid, containing carboxyl, phenolic and amine groups, they increased the adsorption of metal ions through surface complexation.

3.2.2. Influence of pH and salt concentration on adsorption

It can be seen from Fig. 8a that the pH value of the solution was an important factor in determining the HA adsorption capacity. With the increase of pH value from 2 to 6, the adsorption capacity of CS-PVA membrane on HA increased from 28.4 to 78.4 $mg \cdot g^{-1}$, the pH value increased from 6 to 12, and the adsorption capacity dropped to 9.67 $mg \cdot g^{-1}$. It could be seen from the structural formula of humic acid that humic acid was a complex network structure connected by functional groups through the aromatic ring as the center, and participates in the adsorption process through the carboxyl group and phenolic hydroxyl group on the humic acid [31]. The appearance of carboxyl and phenolic hydroxyl groups was affected by the pH of the solution, and the configuration of HA changed with the pH of the solution. When the pH of the solution was 6, the number of anions and cations dissociated from the humic acid in the solution was almost the same. At this time, the adsorption of humic acid by the membrane reached the maximum. With the increase of acidity, the electrostatic repulsion increased and the amount of adsorption decreases [32]. Humic acid existed in a spherical structure when the pH was low, and existed in a linear or tensile structure when the pH was high [33]. Therefore, as the pH

Table 1
Adsorption models selected in this study

Name of the models	Expressions	Parameter description
Langmuir model	$q_e = \frac{q_m K_L C_e}{1 + K_L C_e}$	K_L ($L \cdot mg^{-1}$) is a constant related to binding energy; q_m ($mg \cdot g^{-1}$) is the theoretical saturated adsorption capacity
Freundlich model	$q_e = K_F C_e^{1/n}$	K_F and $1/n$ are parameters of this model
Koble–Corrigan model	$q_e = \frac{AC_e^{\ n}}{1 + BC_e^{\ n}}$	A, B and n are all equation parameters
Pseudo-second-order equation	$q_t = \frac{k_2 q_e^2 t}{1 + K_2 q_e t}$	k_2 ($g \cdot mg^{-1} \cdot min^{-1}$) is the rate constant
Elovich equation	$q_t = A + B \ln t$	A and B are parameters of model
Double constant equation	$\ln q_t = \ln A + K_{st}$	A and K_{st} are parameters of model

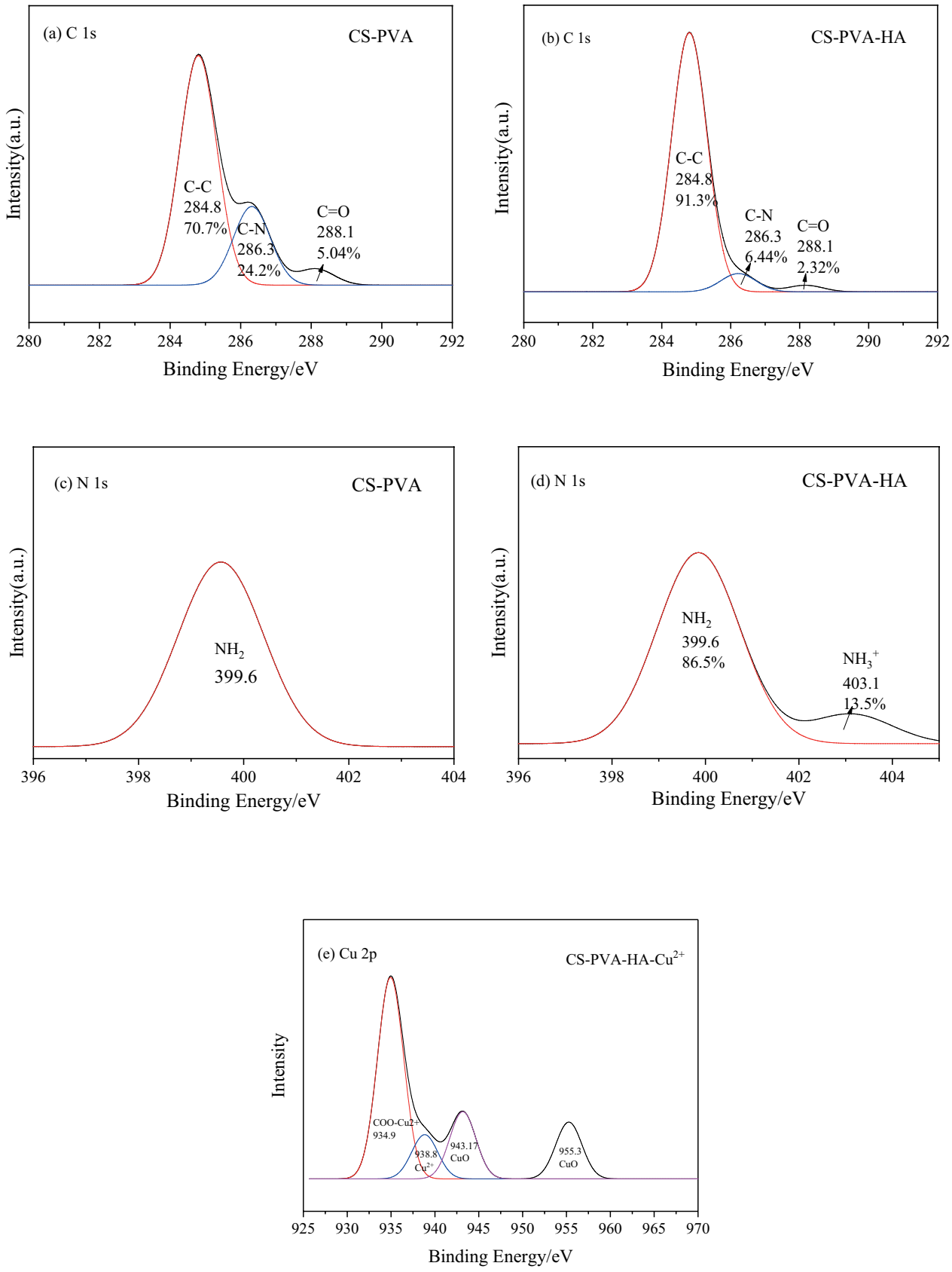

Fig. 6. Fractional peak plots of C 1s and N 1s before and after the adsorption of HA and Cu^{2+} by CS-PVA (CS-PVA-HA) membrane. (a, c) for CS-PVA, (b, d) for CS-PVA-HA, and (e) for Cu^{2+}.

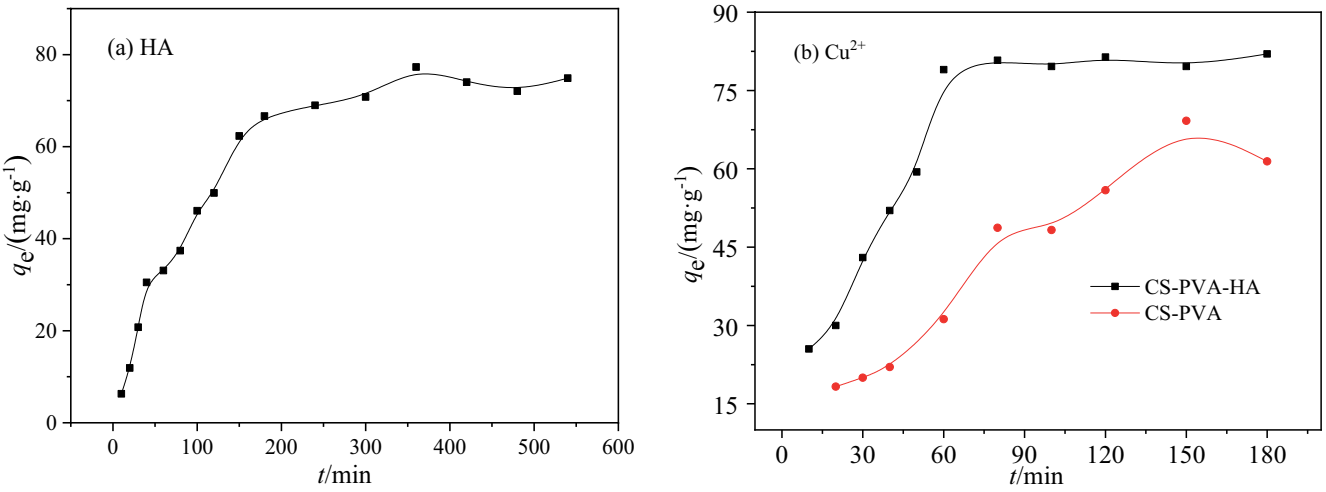

Fig. 7. Effect of time and adsorbent dosage on the adsorption of HA (a) and Cu^{2+} (b) (for HA, C_0 = 150 mg·L^{-1}, T = 303 K, t = 360 min; for Cu^{2+}, C_0 = 200 mg·L^{-1}, T = 303 K, t = 60 min).

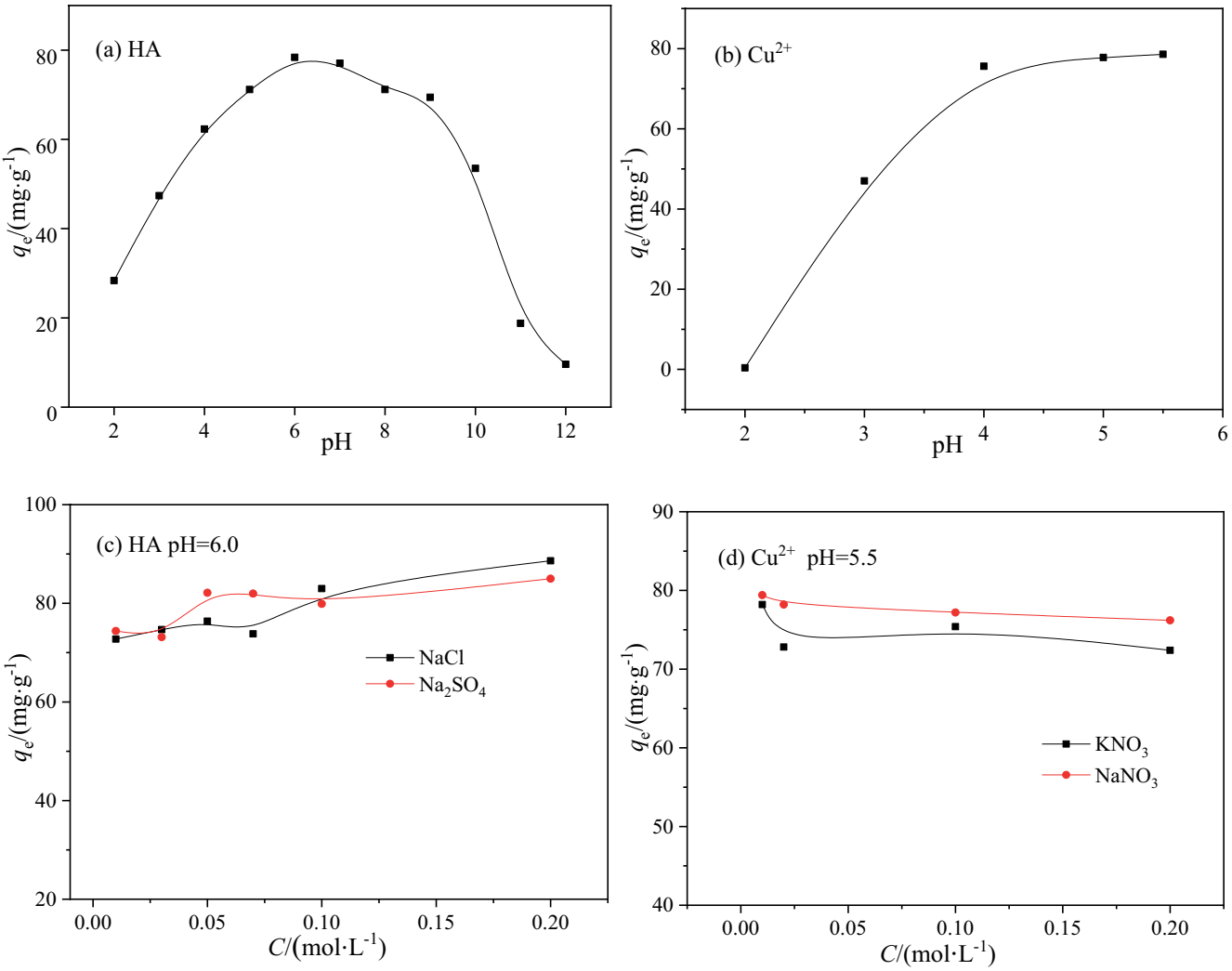

Fig. 8. Effect of pH and salt concentration on the adsorption of HA and Cu^{2+} (a, c) for HA, C_0 = 150 mg·L^{-1}, T = 303 K and (b, d) Cu^{2+}, C_0 = 200 mg·L^{-1}, T = 303 K.

value of the solution increased, the molecular size of humic acid increased, which would also cause the adsorption capacity to decrease when the pH value increased. And chitosan was hydrophobic in a neutral solution, which was conducive to the adsorption of humic acid. Therefore, the best adsorption pH of CS-PVA to HA was 6 [32].

It can be seen from Fig. 8b that the adsorption of Cu^{2+} by the CS-PVA-HA membrane was greatly affected by the pH of the solution. When the pH value increased from 2 to 5.5, the adsorption capacity increased from 0.5 to 78.6 mg·g^{-1}. When the pH was between 4 and 5.5, the adsorption capacity remained basically unchanged. When the pH value was low, the groups on the surface of the humic acid would react with H^+ and occupy the adsorption sites, making the surface of the CS-PVA-HA membrane positively charged. Cu^{2+} existed in the form of $[Cu(H_2O)_6]^{2+}$, and the repulsive force between Cu^{2+} and the film weakens the adsorption of Cu^{2+} [34]. Therefore, as the pH value increased, the adsorption of H^+ in the solution weakened, and the adsorption of Cu^{2+} increased significantly. When the pH value kept increasing, humic acid could be used as the carrier of Cu^{2+} hydrolyze, and the adsorption capacity gradually increased to a stable level. Solution pH 5.5 was the best [35].

As shown in Fig. 8c, as the salt concentration increased, the adsorption capacity increased. When the concentration of NaCl and Na_2SO_4 in the solution increased to 0.2 mol·L^{-1}, the adsorption capacity of the CS-PVA membrane on humic acid increased from 73.5 mg·g^{-1} to 84.6 mg·g^{-1} and 88.9 mg·g^{-1}, respectively. This was mainly because the salting-out effect reduced the solubility of humic acid in water. During salting-out, the decrease of solubility in water facilitated the diffusion of humic acid to the surface of the adsorbent and increased the adsorption capacity. The combination of ions and active groups on the HA molecule compressed the electric double layer, the electron cloud density on HA decreased, the repulsive force between the HA colloidal particles and the molecules decreased, and the HA colloidal particles polymerize, making it easier for HA to adsorb CS-PVA film surface [36]. It can be seen from Fig. 8d that the Cu^{2+} adsorption capacity of the CS-PVA-HA film decreased with the increase of the salt concentration. When the salt concentration increased from 0.01 to 0.2 mol·L^{-1} in the solution, the adsorption capacity decreased from 81.6 mg·g^{-1} to 72.4 and 76.8 mg·g^{-1}, respectively. The main reason was that the pH value was small and the membrane surface had more negative charges. The effect of K^+, Na^+ and negative charges in the solution reduced the stability and the adsorption sites were occupied, thereby reducing the adsorption capacity [37]. Therefore, the coexisting ions had a positive effect on the adsorption of humic acid on the CS-PVA membrane, and had a negative effect on the adsorption of Cu^{2+} on the CS-PVA-HA membrane.

3.2.3. Adsorption isotherm analysis

Analysis of isotherm data can predict the adsorption capacity and adsorption behavior of the adsorbent. It can be seen from Fig. 9a that as the equilibrium concentration increased, the unit adsorption q_e gradually increased. It might be because as the initial concentration of humic acid increased, the concentration gradient on the surface of the CS-PVA membrane increased, so that the active sites on the adsorption surface could combine with the adsorbate until it reached a saturated state. With the increase of temperature, the unit adsorption capacity of the same concentration of humic acid decreased, indicating that the adsorption of humic acid by CS-PVA membrane was an exothermic process.

Adsorption isotherm models, Langmuir model, Freundlich model and Koble–Corrigan model are used to fit the equilibrium data using nonlinear regressive analysis. The expressions of three models are listed in Table 1. The fitting results are shown in Fig. 9a and Table 2. For HA adsorption, the values of q_m from Langmuir model were very close to the data of experiments. The R^2 obtained by Langmuir model was above 0.910, and the SSE value was relatively small. Furthermore, it was also found that the fitted curves from Langmuir model were closer to the experimental points. The adsorption process of the CS-PVA film on HA was more in line with the Langmuir model, and it also showed that the reaction was a monolayer adsorption

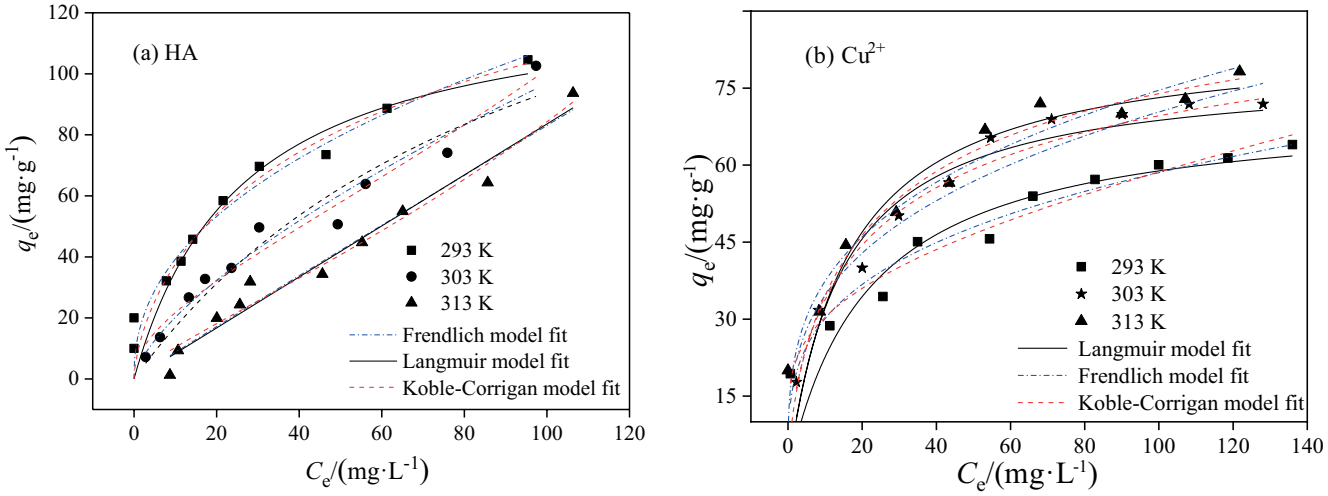

Fig. 9. Isotherms and fitted curves of HA (a) and Cu^{2+} (b) adsorption.

Table 2
Isotherms and fitted parameters of HA and Cu^{2+} adsorption

			Langmuir			
	T (K)	K_L (L·mg^{-1})	$q_{e(exp)}$ (mg·g^{-1})	$q_{m(theo)}$ (mg·g^{-1})	R^2	SSE
HA	293	0.0381 ± 0.0111	104	108 ± 15	0.919	597
	303	0.00995 ± 0.00388	102	101 ± 46	0.943	384
	313	3.78E-7 ± 0	93.7	93.1 ± 8.1	0.965	216
Cu	293	0.04615 ± 0.01806	63.7	71.6 ± 7.4	0.797	376
	303	0.0691 ± 0.011	71.8	78.7 ± 3.8	0.944	156
	313	0.0617 ± 0.0214	72.7	85.0 ± 7.4	0.840	485
			Koble–Corrigan			
	T (K)	A	B	n	R^2	SSE
HA	293	9.80 ± 8.54	0.0480 ± 0.0265	0.672 ± 0.434	0.913	558
	303	6.44 ± 2.10	0.0728 ± 0.1248	0.433 ± 0.223	0.966	202
	313	1.78 ± 1.47	–0.0131 ± 0.324	0.733 ± 0.307	0.964	193
Cu	293	9.91 ± 9.68	–0.478 ± 0.572	0.0947 ± 0.1331	0.961	62.7
	303	11.6 ± 3.5	0.114 ± 0.023	0.641 ± 0.156	0.962	92.5
	313	10.6 ± 12.6	0.101 ± 0.072	0.688 ± 0.553	0.825	464
			Freundlich			
	T (K)	K_F	1/n	R^2		SSE
HA	293	14.2 ± 3.3	0.441 ± 0.061	0.921		579
	303	4.20 ± 1.00	0.681 ± 0.057	0.963		246
	313	0.913 ± 0.326	0.979 ± 0.082	0.965		214
Cu	293	15.5 ± 1.9	0.289 ± 0.029	0.951		90.7
	303	17.0 ± 2.3	0.308 ± 0.032	0.942		162
	313	18.7 ± 4.9	0.300 ± 0.062	0.836		498

on a uniform surface. Of course, Freundlich model and Koble–Corrigan model were also suitable to describe the process of equilibrium according to values of R^2 and SSE listed in Table 1.

For Cu^{2+} adsorption, it can be seen from Fig. 9b that as the equilibrium concentration increased and the temperature increased, the unit adsorption amount q_e gradually increased, and the unit adsorption amount of Cu^{2+} at the same concentration increased. This shows that the adsorption of Cu^{2+} by CS-PVA-HA film was an endothermic process [38].

Models were used to perform nonlinear fitting on the experimental data of CS-PVA-HA film adsorption of Cu^{2+}. The fitting results are shown in Fig. 9b and Table 2. It could be seen that the theoretical adsorption data obtained by the Langmuir model was deviated from the experimental data, and the R^2 was smaller, and the SSE was larger compared with Freundlich model and Koble–Corrigan model, this inferred that this model was not suitable for describing the model. The SSE of the Freundlich model was small, and the K_F value increased as the temperature increased, indicating that the adsorption of Cu^{2+} by the CS-PVA-HA film was an endothermic process. The value of 1/n was between 0.2 and 0.3, indicating that the adsorption process is easy to carry out. Therefore, the adsorption of Cu^{2+} by the CS-PVA-HA film conformed to the Freundlich model, the multi-molecular layer adsorption process on the uneven surface.

3.2.4. Adsorption kinetic analysis

One of the important properties of adsorbents was adsorption capacity. It can be seen from Fig. 10a and e that as the concentration of HA increased, the amount of adsorption gradually increased. This might be due to the increase in the concentration of HA solution providing a greater driving force for the adsorbate to overcome the mass transfer resistance between the water phase and the solid phase. When the initial concentration of the solution increased, the number of adsorbate molecules increased, and the probability of collision and binding with the adsorbent sites increased, and the adsorption capacity increased accordingly. With the increase of temperature, the adsorption capacity of CS-PVA film on HA decreased from 104 to 93.7 mg·g^{-1}, and the equilibrium adsorption capacity decreased with the increase of temperature. This showed that the adsorption of HA by CS-PVA film was an exothermic process. Pseudo-second-order kinetic, Elovich, double constant models are used to fit the kinetic data of HA and the expressions are also listed in Table 1. The fitted curves and parameters are shown in Fig. 10a, c, e and Table 3a, respectively. The R^2 obtained by Elovich model fitting

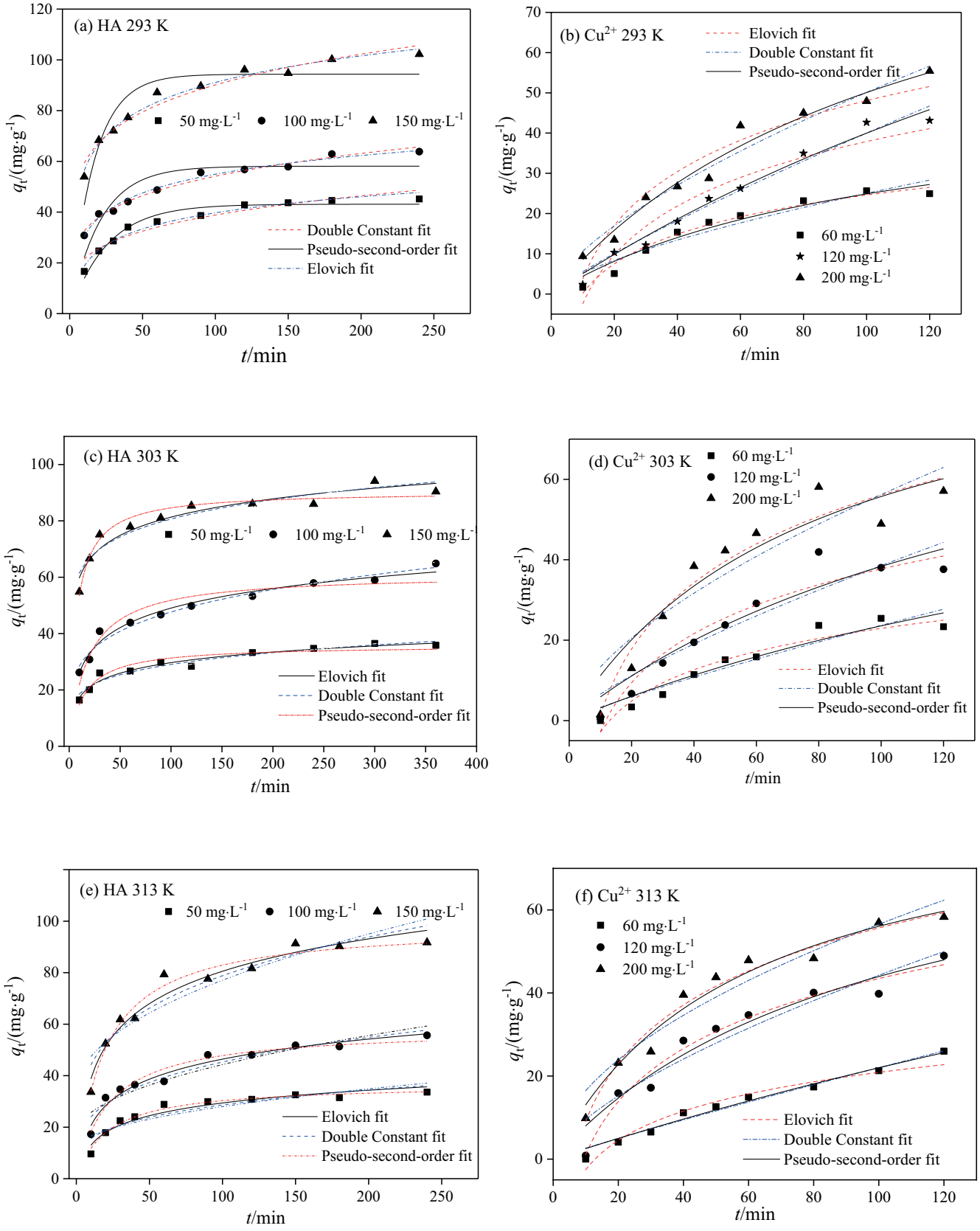

Fig. 10. Kinetic nonlinear fitting curves of adsorption for HA (a, c, e) and Cu^{2+} (b, d, f).

Table 3a
Results of nonlinear fitting of kinetic curves for HA adsorption

Elovich equation					
T (K)	C_0 (mg·L^{-1})	A	B	R^2	SSE
293	50	–2.40 ± 2.29	9.15 ± 0.54	0.970	22.3
	100	5.89 ± 1.90	10.6 ± 0.4	0.984	15.4
	150	21.6 ± 3.0	15.1 ± 0.7	0.981	38.4
303	50	4.77 ± 1.81	5.41 ± 0.39	0.954	16.7
	100	2.91 ± 2.63	10.0 ± 0.6	0.971	35.0
	150	38.3 ± 4.1	9.35 ± 0.90	0.922	85.3
313	50	–3.49 ± 3.90	7.14 ± 0.68	0.924	35.5
	100	–3.52 ± 3.23	11.2 ± 0.8	0.960	44.3
	150	–5.36 ± 5.8	18.2 ± 1.4	0.951	145
Double constant model					
T (K)	C_0 (mg·L^{-1})	A	k_s	R^2	SSE
293	50	11.9 ± 1.6	0.257 ± 0.280	0.920	59.3
	100	19.6 ± 1.0	0.221 ± 0.012	0.979	20.7
	150	46.8 ± 3.2	0.118 ± 0.014	0.897	115
303	50	11.8 ± 1.1	0.195 ± 0.018	0.0937	22.7
	100	6.63 ± 0.24	0.111 ± 0.007	0.964	0.607
	150	10.4 ± 0.2	0.0670 ± 0.0036	0.978	0.271
313	50	8.44 ± 1.66	0.265 ± 0.042	0.847	71.7
	100	12.7 ± 1.8	0.277 ± 0.029	0.924	85.8
	150	24.8 ± 3.5	0.251 ± 0.030	0.904	284
Pseudo-second-order kinetic model					
T (K)	C_0 (mg·L^{-1})	$q_{e(\exp)}$ (mg·g^{-1})	$q_{e(\text{theo})}$ (mg·g^{-1})	k_2 (g·mg^{-1}·min^{-1})	R^2	SSE
293	50	45	49.1 ± 0.7	0.00102 ± 6.89E-5	0.992	6.02
	100	63	64.7 ± 2.0	0.00105 ± 1.895E-4	0.924	74.8
	150	102	103 ± 2	8.90E-4 ± 1.07E-4	0.959	81.5
303	50	36	35.8 ± 1.2	0.00195 ± 3.9316E-4	0.906	33.8
	100	60	61.2 ± 2.3	9.069 E-4 ± 2.000E-4	0.902	119
	150	92	90.5 ± 1.4	0.0016 ± 2.007E-4	0.923	63.7
313	50	33	36.7 ± 0.9	0.0129 ± 1.569E-4	0.977	10.8
	100	55	58.3 ± 1.9	7.79E-4 ± 1.29E-4	0.955	50.2
	150	90	98.7 ± 2.5	5.31E-4 ± 0.68E-4	0.970	88.4

was greater than 0.920, but the SSE was too large at 313 K, which was not suitable for describing the adsorption of HA by CS-PVA membrane. The R^2 of pseudo-second-order kinetic model was greater than 0.920 and the SSE is smaller, and the fitted curves were closest to experimental point. So it can be inferred that this model be most suitable to describe the adsorption of HA by CS-PVA membrane. This was similar to the results of Liao et al. [39], indicating that this adsorption process contained chemical adsorption and chemical adsorption was a rate-controlling process.

It can be seen from Fig. 10b, d, f that as the Cu^{2+} concentration increased, the adsorption capacity gradually increased. Models such as Elovich, pseudo-second-order kinetic, double constant are used to fit the Cu^{2+} kinetic data. The fitted results are also shown in Fig. 10 and Table 3b. The theoretical data of the pseudo-second-order kinetic model was deviated from the experimental data. The R^2 of the Elovich equation were greater than 0.92, and the SSE was smaller, while the fitted curves from this model were closest to experimental points. Therefore, the Elovich equation was more suitable for the adsorption process. The adsorption process might be the complexation of the functional groups COOH and –OH with Cu^{2+}, or the complexation of two –COOH with Cu^{2+} [40]. Because the phenolic hydroxyl group –OH (pK_a 8–11) did not dissociate at pH 5.5, the carboxyl group might be the main functional group for Cu^{2+} adsorption on the CS-PVA-HA membrane. Increasing the carboxyl content of the CS-PVA-HA film could increase the adsorption capacity of the CS-PVA-HA film to Cu^{2+}.

Table 3b
Results of nonlinear fitting of kinetic curves for Cu^{2+} adsorption

Elovich equation					
T (K)	C_0 (mg·L^{-1})	A	B	R^2	SSE
293	60	–24.3 ± 2.5	10.6 ± 0.6	0.972	14.4
	120	–42.8 ± 6.4	17.5 ± 1.7	0.931	99.1
	200	–40.6 ± 7.2	19.3 ± 1.9	0.930	125
303	60	–28.8 ± 4.2	11.2 ± 1.1	0.930	42.3
	120	–43.3 ± 6.7	17.6 ± 1.7	0.927	108
	200	–53.5 ± 8.5	23.8 ± 2.2	0.936	172
313	60	–26.0 ± 3.2	10.2 ± 0.8	0.948	25.0
	120	–41.3 ± 4.3	18.4 ± 1.1	0.971	44.3
	200	–37.5 ± 4.9	20.2 ± 1.3	0.969	57.8
Double constant model					
T (K)	C_0 (mg·L^{-1})	A	k_s	R^2	SSE
293	60	1.09 ± 0.48	0.680 ± 0.100	0.903	50.3
	120	0.772 ± 0.231	0.857 ± 0.067	0.972	41.4
	200	2.25 ± 0.60	0.674 ± 0.060	0.958	73.8
303	60	0.455 ± 0.289	0.858 ± 0.142	0.891	65.4
	120	1.12 ± 0.71	0.769 ± 0.142	0.863	203
	200	3.16 ± 1.81	0.625 ± 0.131	0.821	482
313	60	0.313 ± 0.106	0.923 ± 0.076	0.970	14.4
	120	2.08 ± 0.88	0.665 ± 0.097	0.903	151
	200	4.81 ± 1.38	0.535 ± 0.066	0.921	149
Pseudo-second-order kinetic model					
T (K)	C_0 (mg·L^{-1})	$q_{e(\exp)}$ (mg·g^{-1})	$q_{e(\text{theo})}$ (mg·g^{-1})	k_2 (g·mg^{-1}·min^{-1})	R^2	SSE
293	60	23	51.4 ± 10.9	1.82E-4 ± 1.05E-4	0.944	28.9
	120	43	171 ± 58.1	1.79E-5 ± 1.38E-5	0.979	30.2
	200	55	109 ± 17	7.79E-5 ± 3.25E-5	0.968	55.8
303	60	24	85.4 ± 54.2	4.46E-5 ± 6.57E-4	0.911	53.8
	120	44	99.6 ± 43.5	6.29 E-5 ± 6.86E-5	0.895	115
	200	57	100 ± 25	1.26E-4 ± 92.05E-4	0.883	315
313	60	25	150 ± 103	1.14E-5 ± 1.67E-5	0.974	12.7
	120	48	87.7 ± 18.7	1.15E-4 ± 0.67E-4	0.935	101
	200	58	88.2 ± 8.3	1.97E-4 ± 5.86E-4	0.964	68.1

3.2.5. Adsorption thermodynamic parameters

Thermodynamic parameters can reflect the changes in the internal energy associated with the adsorption process, which often has the characteristics of exothermic, endothermic, and system changes [36]. The mechanism of the adsorption reaction can also be analyzed from the internal energy changes. The Gibbs free energy change (ΔG), enthalpy change (ΔH) and entropy change (ΔS) are used to explain the spontaneity of the adsorption process, the energy change and the increase or decrease of the disorder. The calculation formula of thermodynamic parameters is as follows:

$$K_c = \frac{C_{\text{ad},e}}{C_e} \tag{2}$$

$$\Delta G = -RT\ln K_c \tag{3}$$

$$\Delta G = \Delta H - T\Delta S \tag{4}$$

where $C_{\text{ad},e}$ is the concentration of HA on the CS-PVA film in adsorption equilibrium (or Cu^{2+} concentration on the CS-PVA-HA film), C_e is the concentration of HA in equilibrium (or Cu^{2+} concentration), R (8.314 J·mol^{-1}·K^{-1}) is the ideal gas constant, T (K) is the adsorption reaction temperature, K_c is the apparent adsorption constant, and ΔG is the Gibbs free energy change.

For the actual system, it is estimated that the degree of difficulty of the adsorption reaction can also be the size of the apparent activation energy E_a (kJ·mol^{-1}). It is often believed that the smaller the value, the easier the adsorption reaction will occur. Its expression is as follows:

$$\ln k = -\frac{E_a}{RT} + \ln A \quad (5)$$

where A is the temperature influence factor, k is the adsorption rate constant.

The thermodynamic parameters and activation energy data of the CS-PVA film adsorption of HA and CS-PVA-HA film adsorption of Cu^{2+} are calculated respectively in Table 4. It could be seen from the data that $\Delta G < 0$, $\Delta H < 0$, and $\Delta S < 0$ indicated that the adsorption of HA by the CS-PVA film was a process of spontaneous, exothermic, and entropy reduction. And the low temperature conditions were conducive to the reaction. Value of E_a (48.5 kJ·mol^{-1}) indicated that the process of CS-PVA membrane adsorption of HA was chemical adsorption. Negative value of ΔS (–81.7 J·mol^{-1}·K^{-1}) might be due to the reduction of the degree of confusion on the solid–liquid interface during the adsorption of HA on the surface of the CS-PVA film in the aqueous solution; on the other hand, it might be due to the HA molecules being adsorbed on the CS-PVA film, its movement was restricted and the entropy is reduced. The parameters in the table showed that the adsorption of Cu^{2+} by the CS-PVA-HA film was a spontaneous process of endothermic entropy increase, and the experimental process included both physical adsorption and chemical adsorption [41].

3.2.6. Comparison of the adsorption capacity of different adsorbents

As can be seen from Table 5a and b, by comparing the adsorption amounts of HA adsorbed by different types of adsorbents, the CS-PVA membrane has a clear advantage. The adsorption capacity of CS-PVA membrane for HA is significantly higher than other adsorbents, which has some potential application value. Different adsorbents were used to adsorb Cu^{2+} and were found to have different adsorption capacities, with the CS-PVA-HA membrane showing the best adsorption effect.

3.2.7. Adsorption mechanism

Chitosan contains a large number of amino and hydroxyl groups. Firstly, the amino group is protonated and subsequently combined with carboxyl or phenolic groups in humic acid by electrostatic gravitational force and hydrogen bonding [50,51]. The adsorption mechanism of HA is shown in Fig. 11a. The prepared CS-PVA-HA membrane showed good adsorption performance on Cu^{2+}, and it was evident from XPS analysis that Cu^{2+} was successfully adsorbed on. The prepared CS-PVA-HA improved the interaction force of functional groups on the chitosan surface due to the addition of HA [50]. The process of adsorption of Cu^{2+} is mainly complexed with COO– of humic acid [52]. The mechanism diagram of Cu^{2+} adsorption is shown in Fig. 11b.

4. Conclusion

The CS-PVA film was obtained by mixing chitosan and polyvinyl alcohol. The experimental results showed that the CS-PVA film had good adsorption performance for HA. The adsorption was best when the pH of the solution is 6, and the coexisting ions had a positive effect on the adsorption. The Langmuir model could describe the adsorption process well. The thermodynamic parameters indicated that the adsorption of HA by the CS-PVA film was a spontaneous, exothermic, and entropy-decreasing chemical adsorption process. Compared with other adsorbents, the prepared CS-PVA-HA film had the strongest Cu^{2+} adsorption capacity and could effectively remove metal ions in water. The secondary adsorption was best when the pH of the solution was 5.5, and the coexisting ions had a negative effect on the adsorption. The Freundlich model was suitable

Table 5a
Comparison of the adsorption capacity of different adsorbents for HA

Adsorbent	q_m (mg·g^{-1})	References
CS-PVA	111	This text
Activated carbon	89.6	[42]
Activated carbon supported chitosan	5.0	[43]
Magnetic resin	3.71	[44]
Medical stone	1	[45]

Table 5b
Comparison of the adsorption capacity of different adsorbents for Cu^{2+}

Adsorbent	q_m (mg·g^{-1})	References
CS-PVA-HA	85.0	This text
TOCN-PEI	52.3	[46]
Fe_5C_2@SiO_2	37.7	[47]
Hordein	64.9	[48]
Corncob	14.3	[49]

Table 4
Thermodynamic parameters of HA (Cu^{2+}) adsorption by CS-PVA (CS-PVA-HA) membranes

				ΔG (kJ·mol^{-1})		
	E_a (kJ·mol^{-1})	ΔH (kJ·mol^{-1})	ΔS (J·mol^{-1}·K^{-1})	293 K	303 K	313 K
HA	48.5	–54.1	–81.7	–3.44	–1.76	–0.369
Cu^{2+}	14.2	13.9	55.8	–2.26	–3.39	–3.38

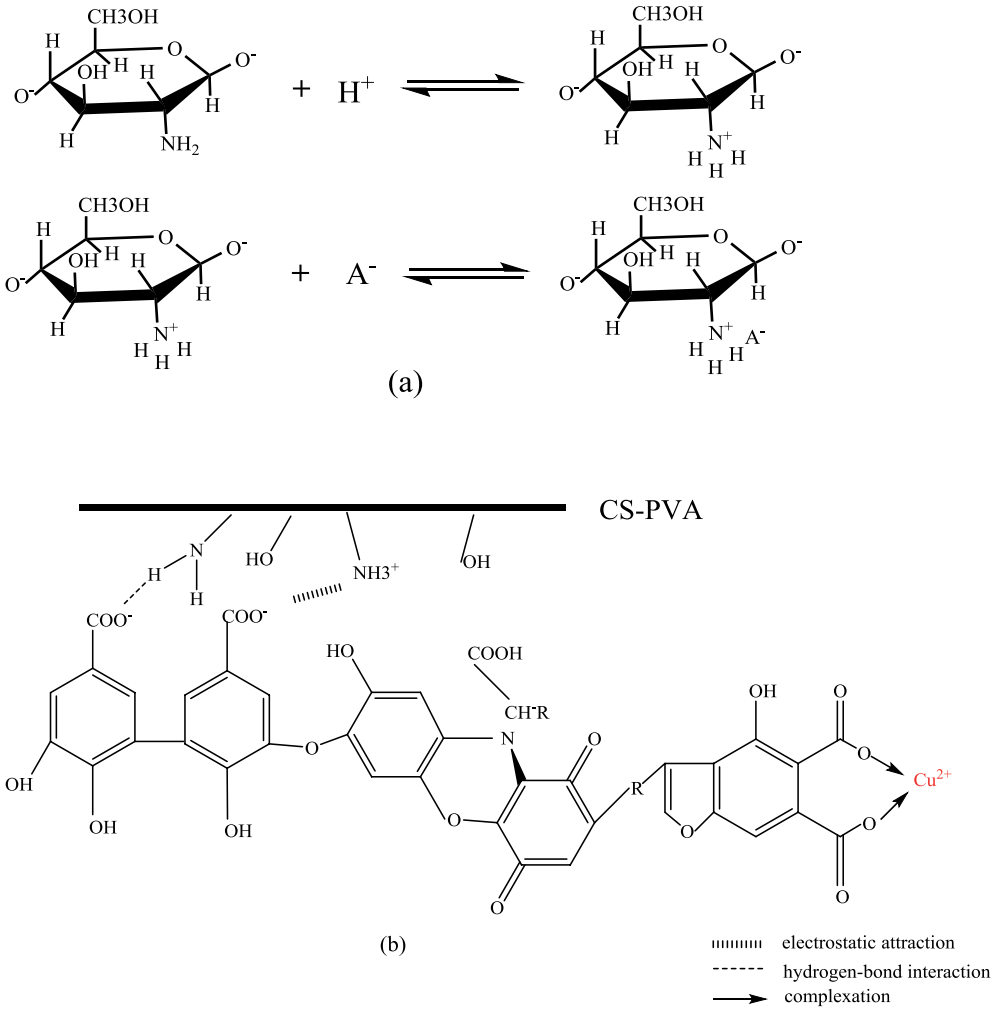

Fig. 11. Mechanism diagram of adsorption of HA onto CS-PVA (a) and Cu^{2+} onto CS-PVA-HA (b).

for describing the adsorption process. According to the parameters, it was inferred that the process was a process of multi-molecular layer adsorption on the uneven surface, and the adsorption mainly depended on the force of complexation. The adsorption was a spontaneous, endothermic, and entropy chemical adsorption process. Therefore, the prepared CS-PVA membrane could adsorb humic acid in water once, and the obtained CS-PVA-HA membrane could adsorb Cu^{2+} through second adsorption. Therefore, it had great application prospects in wastewater treatment.

References

[1] E.A. Paul, The nature and dynamics of soil organic matter: plant inputs, microbial transformations, and organic matter stabilization, Soil Biol. Biochem., 98 (2016) 109–126.
[2] Y. Zha, Y. Wang, S. Liu, Y. Yang, H. Jiang, Y. Zhang, Adsorption characteristics of organics in the effluent of ultra-short SRT wastewater treatment by single-walled, multi-walled, and graphitized multi-walled carbon nanotubes, Sci. Rep., 8 (2018) 17245, doi: 10.1038/s41598-018-35374-8.
[3] S. Yang, L. Li, Z. Pei, C. Li, X. Shan, Effects of humic acid on copper adsorption onto few-layer reduced graphene oxide and few-layer graphene oxide, Carbon, 75 (2014) 227–235.
[4] X. Zhang, Y. Li, Y. Hou, Preparation of magnetic polyethylenimine lignin and its adsorption of Pb(II), Int. J. Biol. Macromol., 141 (2019) 1102–1110.
[5] Y. Zhou, J. Lu, Y. Zhou, Y. Liu, Recent advances for dyes removal using novel adsorbents: a review, Environ. Pollut., 252 (2019) 352–365.
[6] F. Mashkoor, A. Nasar, Magsorbents: Potential candidates in wastewater treatment technology – a review on the removal of methylene blue dye, J. Magn. Magn. Mater., 500 (2020) 166408, doi: 10.1016/j.jmmm.2020.166408.
[7] A.A. Aryee, F.M. Mpatani, E. Dovi, Q. Li, J. Wang, R.P. Han, Z. Li, L.B. Qu, A novel antibacterial biocomposite based on magnetic peanut husk for the removal of trimethoprim in solution: adsorption and mechanism study, J. Cleaner Prod., 329 (2021) 129722, doi: 10.1016/j.jclepro.2021.129722.
[8] A. Shafique, Removal of toxic pollutants from aqueous medium through adsorption: a review, Desal. Water Treat., 234 (2021) 38–57.
[9] F.M. Mpatani, A.A. Aryee, A.N. Kani, R.P. Han, Z.H. Li, E. Dovi, L.B. Qu, A review of treatment techniques applied for selective removal of emerging pollutant-trimethoprim from aqueous systems, J. Cleaner Prod., 308 (2021) 127359, doi: 10.1016/j.jclepro.2021.127359.
[10] K. Li, P. Li, J. Cai, S. Xiao, H. Yang, A. Li, Efficient adsorption of both methyl orange and chromium from their aqueous mixtures using a quaternary ammonium salt modified chitosan magnetic composite adsorbent, Chemosphere, 154 (2016) 310–318.

[11] M.Y. Liu, X.T. Zhang, Z.H. Li, L.B. Qu, R.P. Han, Fabrication of zirconium (IV)-loaded chitosan/Fe_3O_4/graphene oxide for efficient removal of alizarin red from aqueous solution, Carbohydr. Polym., 248 (2020) 116792, doi: 10.1016/j.carbpol.2020.116792.
[12] S. Wu, F. Wang, H. Yuan, L. Zhang, S. Mao, Fabrication of xanthate-modified chitosan/poly(N-isopropylacrylamide) composite hydrogel for the selective adsorption of Cu(II), Pb(II) and Ni(II) metal ions, Chem. Eng. Res. Des., 139 (2018) 197–210.
[13] Z. Sutirman, E. Rahim, M. Sanagi, K. Abd Karim, W. Wan Ibrahim, New efficient chitosan derivative for Cu(II) ions removal: characterization and adsorption performance, Int. J. Biol. Macromol., 153 (2020) 513–522.
[14] E. Simsek, D. Saloglu, N. Ozcan, I. Novak, D. Berek, Carbon fiber embedded chitosan/PVA composites for decontamination of endocrine disruptor bisphenol-A from water, J. Taiwan Inst. Chem. Eng., 70 (2016) 291–301.
[15] D.A.S. Rodrigues, J.M. Moura, G.L. Dotto, T.R.S. Cadaval Jr., L.A.A. Pinto, Preparation, characterization and dye adsorption/reuse of chitosan-vanadate films, J. Polym. Environ., 26 (2018) 2917–2924.
[16] S. Yang, L. Li, Z. Pei, C. Li, X. Shan, Effects of humic acid on copper adsorption onto few-layer reduced graphene oxide and few-layer graphene oxide, Carbon, 75 (2014) 227–235.
[17] D. Xu, S. Zhu, H. Chen, F. Li, Structural characterization of humic acids isolated from typical soils in China and their adsorption characteristics to phenanthrene, Colloids Surf., A, 276 (2006) 1–7.
[18] M.Y. Liu, Q. Liu, Z.Y. Zang, R.P. Han, Adsorptive removal of sulfosalicylic acid from aqueous medium by iron(III)-loaded magnetic chitosan/graphene oxide, J. Colloid Interface Sci., 606 (2022) 1249–1260.
[19] L. Fan, Y. Zhang, X. Li, C. Luo, F. Lu, H. Qiu, Removal of alizarin red from water environment using magnetic chitosan with Alizarin Red as imprinted molecules, Colloids Surf., B, 91 (2012) 250–257.
[20] Y. Jiang, J. Gong, G. Zeng, X. Ou, Y. Chang, Magnetic chitosan–graphene oxide composite for anti-microbial and dye removal applications, Int. J. Biol. Macromol., 82 (2016) 702–710.
[21] L. Zhao, F. Luo, J. Wasikiewicz, H. Mitomo, Adsorption of humic acid from aqueous solution onto irradiation-crosslinked carboxymethylchitosan, Bioresour. Technol., 99 (2008) 1911–1917.
[22] X. Wang, Z. Wu, Y. Wang, W. Wang, X. Wang, Adsorption–photodegradation of humic acid in water by using ZnO coupled TiO_2/bamboo charcoal under visible light irradiation, J. Hazard. Mater., 262 (2013) 16–24.
[23] E. Derakhshani, A. Naghizadeh, Optimization of humic acid removal by adsorption onto bentonite and montmorillonite nanoparticles, J. Mol. Liq., 259 (2018) 76–81.
[24] R. Saravanan, M.M. Khan, V.K. Gupta, E. Mosquera, F. Gracia, V. Narayanan, A. Stephen, ZnO/Ag/Mn_2O_3 nanocomposite for visible light-induced industrial textile effluent degradation, uric acid and ascorbic acid sensing and antimicrobial activity, RSC Adv., 5 (2015) 34645–3465.
[25] X. Zhang, R. Bai, Mechanisms and kinetics of humic acid adsorption onto chitosan-coated granules, J. Colloid Interface Sci., 264 (2003) 30–38.
[26] X. Zhou, S. Zhou, F. Ma, Y. Xu, Synergistic effects and kinetics of rGO-modified TiO_2 nanocomposite on adsorption and photocatalytic degradation of humic acid, J. Environ. Manage., 235 (2019) 293–302.
[27] L. Zhao, X. Lv, K. Huang, S. Li, J. Liu, Y. Yan, R.Q. Duan, Adsorption of Cu(II) by phosphogypsum modified with sodium dodecyl benzene sulfonate, Int. J. Biol. Macromol., 387 (2019) 121808, doi: 10.1016/j.ijbiomac.2019.05.107.
[28] Y. Zhou, Y. He, Y. Xiang, S. Meng, X. Liu, Single and simultaneous adsorption of pefloxacin and Cu(II) ions from aqueous solutions by oxidized multi-walled carbon nanotube, Sci. Total Environ., 646 (2019) 29–36.
[29] Y. Zhou, Y. Zhang, G. Li, Y. Wu, T. Jiang, A further study on adsorption interaction of humic acid on natural magnetite, hematite and quartz in iron ore pelletizing process: effect of the solution pH value, Powder Technol., 271 (2015) 155–166.
[30] M. Zulfikar, S. Afrita, D. Wahyuningrum, M. Ledyastuti, Preparation of Fe_3O_4-chitosan hybrid nano-particles used for humic acid adsorption, Environ. Nanotechnol. Monit. Manage., 6 (2016) 64–75.
[31] Y. Zhao, W. Zhou, Y. Wang, B. Gao, X. Xu, Y. Zhao, The effect of humic acid and bovine serum albumin on the adsorption and stability of ZnO nanoparticles on powdered activated carbon, J. Cleaner Prod., 251 (2020) 119695, doi: 10.1016/j.jclepro.2019.119695.
[32] C. Hu, M. Wei, J. Chen, H. Liu, M. Kou, Comparative study of the adsorption/immobilization of Cu by turmeric residues after microbial and chemical extraction, Sci. Total Environ., 691 (2019) 1082–1088.
[33] L. Zhao, Q. Zhang, X. Li, J. Ye, J. Chen, Adsorption of Cu(II) by phosphogypsum modified with sodium dodecyl benzene sulfonate, J. Hazard. Mater., 387 (2020) 121808, doi: 10.1016/j.jhazmat.2019.121808.
[34] J. Zhang, H. Yin, L. Chen, F. Liu, H. Chen, The role of different functional groups in a novel adsorption-complexation-reduction multi-step kinetic model for hexavalent chromium retention by undissolved humic acid, Environ. Pollut., 237 (2018) 740–746.
[35] Y. Zhou, Y. He, Y. Xiang, S. Meng, X. Liu, Single and simultaneous adsorption of pefloxacin and Cu(II) ions from aqueous solutions by oxidized multi-walled carbon nanotube, Sci. Total Environ., 646 (2019) 29–36.
[36] F. Ahmadpoor, S. Shojaosadati, S. Mousavi, Magnetic silica coated iron carbide/alginate beads: synthesis and application for adsorption of Cu(II) from aqueous solutions, Int. J. Biol. Macromol., 128 (2019) 941–947.
[37] H. Gao, M. Xiu, M. Wang, B. Zhan, X. Deng, Systematic investigation on the adsorption performance and mechanism of MnO_2/TA nanoflowers for Cu(II) removal from aqueoussolution, ChemistrySelect, 4 (2019) 3247–3258.
[38] X. Guan, X. Lv, K. Huang, Adsorption of Cu(II) ion by a novel hordein electrospun nanofiber modified by β-cyclodextrin, Int. J. Biol. Macromol., 135 (2019) 691–697.
[39] W. Zou, R. Han, Z. Chen, J. Zhang, J. Shi, Kinetic study of adsorption of Cu(II) and Pb(II) from aqueous solutions using manganese oxide coated zeolite in batch mode, Colloids Surf., A, 279 (2006) 238–246.
[40] Y. Liu, T. Li, G. Zeng, B. Zheng, W. Xu, S. Liu, Removal of Pb(II) from aqueous solution by magnetic humic acid/chitosan composites, J. Cent. South Univ., 23 (2016) 2809–2817.
[41] J. Zeng, P. Qi, J. Shi, T. Pichler, F. Wang, Y. Wang, K. Sui, Chitosan functionalized iron nanosheet for enhanced removal of As(III) and Sb(III): synergistic effect and mechanism, Chem. Eng. J., 382 (2020) 122999, doi: 10.1016/j.cej.2019.122999.
[42] H. Eustáquio, C. Lopes, R. Rocha, B. Cardoso, S. Pergher, Modification of activated carbon for the adsorption of humic acid, Adsorpt. Sci. Technol., 33 (2015) 117–126.
[43] S. Maghsoodloo, B. Noroozi, A. Haghi, G. Sorial, Consequence of chitosan treating on the adsorption of humic acid by granular activated carbon, J. Hazard. Mater., 191 (2011) 380–387.
[44] C. Shuang, F. Pan, Q. Zhou, A. Li, P. Li, W. Yang, Magnetic polyacrylic anion exchange resin: preparation, characterization and adsorption behavior of humic acid, Ind. Eng. Chem. Res., 51 (2012) 4380–4387.
[45] H. Yang, B. Luo, Y. Zhang, B. Zhou, S. Manzoor Ahmed, Study of humic acid adsorption character on natural maifan stone: characterization, kinetics, adsorption isotherm, and thermodynamics, ACS Omega, 5 (2020) 7683–7392.
[46] N. Zhang, G. Zang, C. Shi, H. Yu, G. Sheng, A novel adsorbent TEMPO-mediated oxidized cellulose nanofibrils modified with PEI: preparation, characterization, and application for Cu(II) removal, J. Hazard. Mater., 316 (2016) 11–18.
[47] F. Ahmadpoor, S. Shojaosadati, S. Mousavi, Magnetic silica coated iron carbide/alginate beads: synthesis and application for adsorption of Cu(II) from aqueous solutions, Int. J. Biol. Macromol., 128 (2019) 941–947.

[48] X. Guan, K. Huang, S. Li, J. Liu, Y. Yan, R. Duan, Adsorption of Cu(II) ion by a novel hordein electrospun nanofiber modified by β-cyclodextrin, Int. J. Biol. Macromol., 135 (2019) 691–697.
[49] X. Wang, S. Wang, W. Liu, Y. Wang, Q. Hou, J. Wang, M. Jin, J. Li, Y. Chen, Preparation and characterization of activated carbon from lignin-rich enzymatically hydrolyzed corncob residues and its adsorption of Cu(II) ions, Starch-Stärke, 72 (2020) 1900131, doi: 10.1002/star.201900131.
[50] S. Wang, E. Li, J. Li, Z. Du, F. Cheng, Enhanced removal of dissolved humic acid from water using eco-friendly phenylalanine-modified-chitosan Fe_3O_4 magnetic nanoparticles, ChemistrySelect, 5 (2020) 4285–4291.
[51] Z. Liu, S. Zhou, Removal of humic acid from aqueous solution using polyacrylamide/chitosan semi-IPN hydrogel, Water Sci. Technol., 1 (2017) 16–26.
[52] M. Afzal, R. Yue, X. Sun, C. Song, S. Wang, Enhanced removal of ciprofloxacin using humic acid modified hydrogel beads, J. Colloid Interface Sci., 543 (2019) 76–83.